Biomaterials Science

PAPER

Cite this: *Biomater. Sci.*, 2017, **5**, 772

Magnetic nanoparticles for drug targeting: from design to insights into systemic toxicity. Preclinical evaluation of hematological, vascular and neurobehavioral toxicology

Mariela A. Agotegaray,*[a] Adrián E. Campelo,[b] Roberto D. Zysler,[c] Fernanda Gumilar,[b] Cristina Bras,[b] Ariel Gandini,[d] Alejandra Minetti,[b] Virginia L. Massheimer[b] and Verónica L. Lassalle[a]

Received 29th December 2016,
Accepted 8th February 2017

DOI: 10.1039/c6bm00954a

rsc.li/biomaterials-science

A simple two-step drug encapsulation method was developed to obtain biocompatible magnetic nanocarriers for the potential targeted treatment of diverse diseases. The nanodevice consists of a magnetite core coated with chitosan (Chit@MNPs) as a platform for diclofenac (Dic) loading as a model drug (Dic–Chit@MNPs). Mechanistic and experimental conditions related to drug incorporation and quantification are further addressed. This multi-disciplinary study aims to elucidate the toxicological impact of the MNPs at hematological, vascular, neurological and behavioral levels. Blood compatibility assays revealed that MNPs did not affect either erythrosedimentation rates or erythrocyte integrity at the evaluated doses (1, 10 and 100 μg mL^{-1}). A microscopic evaluation of blood smears indicated that MNPs did not induce morphological changes in blood cells. Platelet aggregation was not affected by MNPs either and just a slight diminution was observed with Dic–Chit@MNPs, an effect possibly due to diclofenac. The examined formulations did not exert cytotoxicity on rat aortic endothelial cells and no changes in cell viability or their capacity to synthesize NO were observed. Behavioral and functional nervous system parameters in a functional observational battery were assessed after a subacute treatment of mice with Chit@MNPs. The urine pools of the exposed group were decreased. Nephritis and an increased number of megakaryocytes in the spleen were observed in the histopathological studies. Sub-acute exposure to Chit@MNPs did not produce significant changes in the parameters used to evaluate neurobehavioral toxicity. The aspects focused on within this manuscript are relevant at the pre-clinical level providing new and novel knowledge concerning the biocompatibility of magnetic nanodevices for biomedical applications.

A. Introduction

The convergent fields of nanomaterials and nanomedicine include technology applied to the treatment, diagnosis, monitoring and control of biomedical features. Research into the development of magnetic nanotechnology as devices for delivery and targeting of therapeutic agents has emerged in the last few years. Several efforts have been made to design and obtain magnetic nanodevices, to study the physico-chemical properties and to understand their behavior *in vivo* for their applicability in the biomedical field.[1,2]

The aim of developing magnetic nanoparticles (MNPs) as targeted delivery platforms lies in the intention to avoid the systemic biodistribution of drugs, a major obstacle for current therapeutics and its subsequent side effects.[3] The implementation of magnetic nanotechnology for drug targeting to a desired site in the body would allow the use of lower drug doses, contributing to an improvement in the treatment of pathologies as well as a lower impact on the environment.

When designing MNPs for targeted drug delivery it is necessary to consider some requirements associated with physicochemical and biocompatibility issues. Regarding physicochemical properties, nano-magnetic based drug delivery systems are desired to exhibit specific characteristics such as: 1 – an appropriate hydrodynamic size and surface charge to enhance the extravasation ability and to avoid uptake by the

[a]*INQUISUR, Departamento de Química, Universidad Nacional del Sur (UNS)-CONICET, Bahía Blanca, Argentina. E-mail: magotegaray@uns.edu.ar*
[b]*Instituto de Investigaciones Biológicas y Biomédicas del Sur (INBIOSUR-CONICET)-UNS Dpto. de Biología, Bioquímica y Farmacia, Universidad Nacional del Sur, Bahía Blanca, Argentina*
[c]*CONICET – Centro Atómico Bariloche, Instituto Balseiro, S.C. de Bariloche, Argentina*
[d]*Instituto de Investigaciones Bioquímicas de Bahía Blanca (INIBIBB-CONICET)-UNS Dpto. de Biología, Bioquímica y Farmacia, Universidad Nacional del Sur, Bahía Blanca, Argentina*

reticuloendothelial system (RES),[4] 2 – monodispersity, to minimize the aggregation of MNPs in dispersion[5] and 3 – superparamagnetism, which is necessary to avoid embolism induced by agglomeration.[6]

Biocompatibility is also essential for the application of magnetic nanodevices in biomedicine. For this purpose, coating of the magnetic core with inorganic and polymeric materials is a useful practice and acts as a support for biomolecules. The toxicity of MNPs on biological entities depends on a wide range of factors related to their intrinsic properties conferred by the structural composition, the dose, the route of administration and the intended use.[7,8] Current concerns and limitations related to the use of nanotechnology in biomedicine lie in the lack of knowledge about the toxicological impact of nanosystems *in vivo*. In the literature there are only a few research studies devoted to the study of MNPs' systemic toxicology. Kim *et al.* investigated the potential toxicity of fluorescent MNPs coated with a 50 nm shell of SiO_2.[9] In their work they studied the biodistribution pattern in mice after 28 days of exposure to the nanodevice and the general toxicological effects employing biochemical markers. The authors concluded that these MNPs do not cause toxicity under the experimental conditions assayed in their work. They also proposed that further research would be required to determine the potential side effects of MNP treatment. This study may be considered as a pioneer work regarding the study of toxicity associated with nanodevices. In the review article published by Ji-Eun Kim *et al.* an exhaustive analysis of the *in vitro* toxicological effects of several MNPs on diverse cell types has been performed.[10] Besides the mentioned references and others in the literature, further multidisciplinary studies on the systemic effects of MNP treatment are still necessary to gain insight into the toxicological effects of magnetic nano-materials intended for drug delivery devices.

In this research work we have developed a novel and simple method for drug loading on chitosan-coated magnetic nanoparticles employing diclofenac as a model drug, on the basis of previous studies.[11,12] All the topics related to the synthesis, the characterization, the size control and the resolution of different problems faced during the development of the nanodevices are reported here. Moreover, considering the potential application of the nanosystems here obtained in the biomedical field, we performed an exhaustive study on the influence of these magnetic systems on different biological models aiming to contribute to the knowledge about the *in vivo* effects. We have studied the effect on human blood considering that blood is the first system that nanoparticles encounter when they enter the body and we also evaluated the impact on endothelial cells to elucidate the cytotoxicity associated with the first barrier that nanoparticles face before arriving to different tissues and organs. Exhaustive research regarding systemic toxicity in mice is also presented revealing interesting results related to toxicity in specific organs. A study which evaluates neurobehavioral toxicity was performed revealing valuable and novel information regarding the impact on the central nervous system. This study represents a novel contribution because it is not commonly employed in the field of magnetic nanoparticle toxicology.

This paper contributes to the knowledge of the impact of magnetic nanoparticles on systemic toxicity and presents a novel conception about the intrinsic and inseparable fields of nanotechnology, biology and medicine when nanosystems are intended for biomedical purposes.

B. Materials and methods

Trypsin/EDTA (10×), L-glutamine (100×), amphotericin B (0.25 mg mL^{-1}) and penicillin/streptomycin (100×) were obtained from Life Technologies (Karlsruhe, Germany). Fetal calf serum was purchased from NATOCOR (Córdoba, Argentina). Griess reagents were purchased from Britania Laboratories (Buenos Aires, Argentina). Dulbecco's modified Eagle's medium (DMEM), diclofenac and all other reagents were purchased from Sigma Chemical Company (St Louis, MO, USA).

B.1. MNP synthesis

The synthesis of the diclofenac-loaded magnetic nanocarrier (Dic–Chit@MNPs) has been carried out in two simple steps as follows: (1) 160 mg of diclofenac sodium were dissolved in aqueous solution of acetic acid (50%) containing the biopolymer chitosan (Chit) (1 mg mL^{-1}). The mixture was stirred at room temperature for 12 hours; (2) a dispersion of nano-magnetite functionalized with oleic acid in acetone, synthesized as previously described in ref. 11, was added drop-wise to the above mixture. The resulting suspension reacted under magnetic stirring at room temperature for two hours, and was then washed three times with distilled water, separated with a high power rare-earth magnet and dried at 45 °C. The supernatant of the reaction was used for diclofenac quantification. The unloaded nanocarrier, named hereafter Chit@MNPs, was synthesized similarly without diclofenac.

B.2. MNP characterization

B.2.1. Diclofenac loading efficiency. The diclofenac loading efficiency was analyzed by a spectrophotometric method adapted from Matin *et al.*[13] Drug loading in the sample was determined indirectly by measurement of the free diclofenac content in the supernatant of the reaction. For this purpose, aliquots were taken and added with 1 mL of HNO_3 (63% w/v). The yellowish compound resulting from the reaction between free diclofenac and nitric acid was quantified by UV-Visible spectroscopy using a Shimadzu 160 Japan spectrophotometer. The same procedure was applied to the supernatant from the unloaded carrier synthesis and was employed as a blank for the reaction. A calibrating curve relating absorbance (A) and diclofenac–HNO_3 concentration was constructed. Drug incorporation was expressed as Diclofenac Encapsulation Efficiency (DEE%): [drug quantified in supernatant (mg)/total drug in the suspension (mg)] × 100.

B.2.2. Iron content. The composition of the nanoparticles in terms of iron content was analyzed by high-resolution inductively coupled plasma atomic emission spectroscopy (ICP-AES, Shimadzu 9000). Samples were prepared by dissolving 10 mg of the magnetic nanoparticles in 10 mL HCl 36% w/v.

B.2.3. FTIR-DRIFTS. Diffuse reflectance infrared Fourier transform spectroscopy (DRIFTS-FTIR) was performed using a Thermo Scientific Nicolet 6700 spectrometer. Spectra were recorded in the range 4000–400 cm^{-1}. Samples were prepared by mixing manually the corresponding powders with KBr (1% w/w).

B.2.4. Hydrodynamic particle diameter (D_h), zeta potential (ζ) and morphology. D_h and ζ measurements were determined by Dynamic Light Scattering (DLS) at 25 °C in a Malvern Zetasizer. Aqueous dispersions were prepared using concentrations of 0.1 mg mL^{-1} of both MNPs. The reported data of D_h and ζ were the resultant from three independent measurements.

Morphology and complementary size data were achieved by Transmission Electron Microscopy (TEM, JEOL100 CXII, JEOL, TOKIO, Japan, 1983 from CCT, Bahía Blanca, Argentina) from aqueous dispersions containing 0.1 mg MNPs per mL.

B.2.5. *In vitro* study of drug release. Diclofenac release was quantified in PBS buffer, pH 7.4 over 24 hours at 37 °C. For such a purpose, 20 mg of Dic–Chit@MNPs were incubated under the influence of a magnetic field or without it. The sample was then separated, dried at 45 °C and evaluated by FTIR spectroscopy to evidence the presence or absence of diclofenac.

B.3. Biological assays

B.3.1. Animals. Primary cultures of ECs were obtained from young Wistar rats (1–2 months old and 150 g of weight). For the *in vivo* biodistribution experimental assays, eight weeks old CF1 female mice were used. All animals were maintained under constant conditions of temperature (22 ± 1 °C) and humidity (70%), in 12 hours light : 12 hours dark cycles during all the experiments. All animals had free access to tap water and standard diet throughout the experiment. The care and handling of the animals were performed in the animal facility from the Biology, Biochemistry and Pharmacy Department of the National University of South in accordance with the internationally accepted standard Guide for the Care and Use of Laboratory Animals as adopted and promulgated by the National Institute of Health.[14] The protocols employed for this study have been approved by the CICUAE (Institutional Committee for the Care and Use of Experimental Animals) belonging to the Biology, Biochemistry and Pharmacy Department of the National University of South.

B.3.2. Effects on endothelial cell culture. Primary cultures of ECs were obtained from aortic ring explants isolated from young Wistar rats.[15] The animals were euthanized and the full length thoracic aorta was aseptically removed. Immediately after, the aorta was cleaned of adherent connective tissue, and cut into small ring-shaped segments. Ring explants were seeded in 60 mm matrix-coated Petri dishes containing DMEM supplemented with 20% (v/v) fetal calf serum (FCS), 60 μg mL^{-1} penicillin, 2.5 μg mL^{-1} amphotericin-B, 2 mM L-glutamine, and 1.7 g L^{-1} sodium bicarbonate. The explants were incubated at 37 °C under a 5% CO_2 atmosphere. In order to establish a pure culture, after three days the ring explants were removed and ECs were allowed to reach confluence. The identity of the ECs was determined by: (a) phase-contrast microscope observation of the characteristic morphology of the cobblestone-shaped growth in the confluent monolayer; (b) positive immunocytochemistry reactivity for CD34 and (c) their ability to synthesize NO.[16] The culture medium was replaced with fresh medium containing 10% (v/v) FCS every 48 hours.

B.3.2.1. NO production measurement on endothelial cells. ECs were seeded on 24-multiwell culture plates at a density of 3.5×10^4 cells per well and allowed to grow to 90% of confluence in DMEM containing 10% (v/v) FCS. Nanoparticle dispersions were prepared using MilliQ® water. Treatments were performed in fresh DMEM containing 2% (v/v) FCS, achieving final concentrations of 1, 10 and 100 μg MNPs per mL medium, performed by triplicate. Controls, where no MNPs were introduced (vehicle alone), were also processed. Nitrites (NO_2^-) were measured in the incubation media as a stable and non-volatile breakdown product of the NO released, employing the spectrometric Griess reaction.[17] Once the treatment was finished, aliquots of the culture medium supernatant were mixed with Griess reagents (1% sulphanilamide and 0.1% naphthylenediamine dihydrochloride in 2.5% phosphoric acid) and incubated for 10 minutes at room temperature. The absorbance was measured at 520 nm in a Biotek Synergy-HT microplate reader. The concentration of NO_2^- in the samples was determined with reference to a sodium nitrite ($NaNO_2$) standard curve performed in the same matrix. Cells were dissolved in 1 M NaOH, and the protein content was measured by the Lowry method.[18] The results are expressed as nmol NO_2^- per mg of protein. To evaluate ECs' response to acetylcholine (ACh) (natural NO production agonist), cells were exposed to 10 μM ACh for 30 minutes.

B.3.2.2. Endothelial cell viability assay. The endothelial cell viability was measured by the MTT assay (Sigma-Aldrich). Cells were seeded onto 96 well plates (1×10^4 cells per well) and incubated for 24 hours in 100 μl of DMEM with 2% FCS. Cells were treated with different concentrations of loaded or unloaded MNPs or vehicle alone for 48 h. After treatment, 10 μl of MTT reagent were added to each sample and the plate was incubated in darkness at 37 °C under a 5% CO_2 atmosphere for 4 hours. After incubation, the medium was removed and 100 μl of DMSO were added to each well. The absorbance was measured at 550 nm in a multiplate reader (Biotek Synergy-HT) using 690 nm as the reference. Results are expressed as optical density (O.D.).

B.3.2.3. Endothelial cells immunofluorescence. ECs were grown on 96-well optical bottom glass-based plates (Nunc Cat. 164588) and exposed to MNP treatment. The cells were processed as previously described.[19] Non-confluent cultures of rat aortic ECs were fixed with 3% paraformaldehyde and permea-

bilized with 0.1% Triton for 5 min. Blocking was performed with 3% albumin in PBS for 30 min. The cells were incubated with Texas Red-phalloidin (Sigma-Aldrich) and the nuclei were counterstained with 4,6-diamidino-2-phenylindole (DAPI) (Sigma-Aldrich). Immunofluorescence was visualized using an Olympus BX41 microscope and recorded with an Olympus QColor 3 digital camera.

B.3.3. Impact of MNPs on human hematological parameters

B.3.3.1. Red blood cell (RBC) morphology and erythrocyte sedimentation rate (ESR). All experiments involving human materials were performed in accordance with the guidelines of Good Clinical Practices (ICH GCP Guidelines), the Helsinki Declaration and Argentine National disposition ANMAT 6677/10 and Buenos Aires provincial law (no. 11044). Informed consent was obtained from all blood donors and, the procedures employed were approved by the National Scientific and Technical Research Council's (CONICET) committee.

Human blood was collected by venous puncture using 5% (v/v) citrate as the anticoagulant. Anticoagulated blood was exposed to diclofenac-loaded or unloaded MNPs at doses of 1, 10 and 100 μg mL^{-1} and incubated for 1 hour at 37 °C. Two controls were also processed: one received no treatment and in the other blood was treated with the vehicle alone. For the morphological study of blood cells, blood smears were prepared immediately after treatment and stained with May Grünwald-Giemsa. Micrographs were taken with a Nikon Eclipse TS100 coupled to a Nikon D3100 Camera at 40×.

The erythrocyte sedimentation rate (ESR) was determined in triplicate for each condition, employing the Westergren ESR methodology[20] at the above-mentioned doses.

B.3.3.2. RBC hemolysis assay. Citrated blood was centrifuged for 10 minutes in a Hermle Z206A centrifuge at 300*g* to separate RBCs and platelet-rich plasma (PRP). RBCs were washed twice with PBS-citrate buffer (pH 7) and centrifuged at 1550*g* for 10 minutes. After the last centrifugation, RBCs were adjusted to 2×10^7 cells per mL and treated with the nanocarrier or diclofenac-loaded nanodevice in final concentrations of 1, 10 and 100 μg mL^{-1} for 60 minutes at 37 °C. After the incubation, samples were centrifuged at 1550*g* for 10 minutes and hemoglobin was determined in supernatants by the hemoglobincyanide method.[21]

B.3.3.3. Platelet aggregation assay. Platelet-rich plasma (PRP) and platelet-poor plasma (PPP) were obtained by sequential centrifugations as previously described.[22] Platelet aggregation was measured using a turbidimetric assay.[23] Briefly 400 μl of PRP (3×10^8 platelets per ml) were exposed to MNPs (100 μg ml^{-1}, 10 μg ml^{-1} or vehicle (control)) for 30 or 15 minutes. Immediately after the treatment, 285 μl of PRP were taken and set in a CronoLog 430 aggregometer cuvette with continuous stirring and aggregation was initiated by the addition of 2×10^{-5} M ADP. Changes in light transmission were recorded for 5 min after ADP addition. The signal generated by PPP was taken as the 100% transparent control.[24] Basal aggregation exhibited by PRP alone, without vehicle or MNP treatment, was considered the maximal aggregation. Results are expressed as percent of platelet aggregation inhibition with respect to the control.

B.4. Toxicity in mice

The experiment was conducted to evaluate the effects of Chit@MNPs as a carrier according to the protocols described by OECD Guideline no. 407 (2008). Healthy eight week old CF1 female mice were randomly divided according to body weight (approximately 30 g) into two groups of eight animals (n = 8). Aqueous dispersions of the magnetic unloaded nanocarrier were administered *via* intraperitoneal (IP) injection once a week over a period of 28 days at a dose of 30 mg per kg body weight. Control animals received the vehicle alone. All the animals were observed for signs of toxicity during the exposure. At the end of the treatment, behavioral and functional parameters were assessed for each mouse and they were subsequently euthanized. Organs such as the liver, spleen, kidneys, stomach, intestine, lungs and brain were extracted and conditioned to perform histopathological examinations.

B.4.1. Functional observational battery. On the 28th day of exposure, behavioral and functional parameters of the animals were evaluated through a functional observational battery. It included a thorough description of the animals' appearance, behavior and functional integrity (US EPA, 1998). Procedural details and scoring criteria for the functional observational battery protocol were performed according to Moser and Ross[25] and modified for mice.[26,27] Briefly, measurements were first carried out in the home cage, where the observer recorded each animal's posture, activity and palpebral closure. The presence or absence of clonic or tonic movements, spontaneous vocalizations and biting were also noted down. The animal was then removed from its cage, rating the ease of removal and handling. All signs of lacrimation, salivation and piloerection were rated. Other abnormal clinical signs were also recorded. The animal was placed in an open field arena having a piece of clean absorbent paper on the surface, and allowed to freely explore for 3 min. During that time, the observer ranked the mouse's arousal, gait score, activity level and rears as well as any abnormal postures, unusual movements, stereotyped behaviors, pelvis elevation and tail position. At the end of the 3 min, the number of fecal boluses and urine pools, and the presence or absence of diarrhea were recorded. Next, sensorial responses were ranked according to a variety of stimuli (click stimulus using a metal clicker, approach and touch rump with a blunt object, pinch of the tail using forceps, and touch of the corner of the eye and the inside of the ear with a fine object). Surface righting reflex and landing foot splay were also evaluated.

In the landing foot splay, the tarsal joint pad of each hindfoot was marked with ink and the animal was then dropped from a height of 15 cm onto a recording sheet. Finally, the wire maneuver was carried out, where the animal was suspended from a horizontal wire by forelimbs and released.

B.4.2. Histopathological examinations. Euthanized animals were macroscopically examined. The liver, spleen, kidneys, stomach, lungs and brain were weighed and the intestine

total length was recorded. Representative fragments of these organs were fixed in formol (10% v/v) solution, dehydrated by serial ethanol solution and enclosed in paraffin. Sections (5 μm thick) (Minot Leica model RS 2165) were stained with hematoxylin–eosin and examined under a light microscope (Olympus Bx51).

B.5. Statistical analysis

Comparisons between two means were performed using Student's *t*-test and multiple comparisons were made by using one way ANOVA, followed by Fisher's least significant difference. *p* values lower than 0.05 were considered to be statistically significant.

In the functional observational battery, descriptive (D) and binary (B) data are expressed as a percentage of incidence and compared by the chi-square test; ranked (R) data are expressed as the mean score of the scale and compared by the Kruskal–Wallis test; continuous (C) data are expressed as the mean value and compared by One-way ANOVA.

C. Results

C.1. Physicochemical properties and mechanism for diclofenac encapsulation

The diclofenac loading efficiency was estimated in 84.0% by UV-Visible spectroscopy. This result is satisfactory in terms of the drug content. The drug loading content resulted in 42.0 (wt%). FTIR spectra corresponding to the carrier and to the diclofenac-loaded nanocarrier are displayed in Fig. 1.

The spectrum corresponding to the nanocarrier presents a band located at 577 cm^{-1}, which is attributable to the Fe–O stretching vibration of magnetite. The bands observed near 2800 cm^{-1} correspond to C–H stretching vibrations from CH_3 and CH_2 groups belonging to chitosan. The peak observable at 1023 cm^{-1} is due to the C–O stretching vibration of the biopolymeric moiety, whereas the wide band at near 3200 cm^{-1} is ascribed to NH and OH groups of the biopolymer.

In the spectrum of Dic–Chit@MNPs bands related to the polymer and magnetite persisted, however a slight shifting is noted when comparing with the bare nanocarrier spectrum.

Furthermore, new bands appear at 1666 cm^{-1} and 1377 cm^{-1} assignable to symmetric and asymmetric stretching vibrations, respectively, of the COO group belonging to diclofenac. Moreover, the band at 1453 cm^{-1} is characteristic of the diclofenac CH_2 bending vibration. Bands near 2900 cm^{-1} present an increased intensity in comparison to the unloaded carrier due to CH_2 and CH stretching vibrations of the drug molecule.

The composition of the magnetic nanocarriers, in terms of the iron content, did not change substantially with the addition of diclofenac. The iron content in the Dic–Chit@MNPs was 0.375 mg mg^{-1} of dry particles, while in the case of Chit@MNPs, reached 0.392 mg mg^{-1} of dry particles.

Magnetization curves corresponding to Chit@MNPs and Dic–Chit@MNPs are displayed in Fig. 2, as a function of the applied magnetic field. From the figure it is evident that the magnetic properties of the nanocarriers were not affected by the diclofenac incorporation since almost similar M_s values were reached in each case (34.7 emu g^{-1} for Dic–Chit@MNPs and 31.7 emu g^{-1} for Chit@MNPs).

TEM micrographs corresponding to Chit@MNPs and Dic–Chit@MNPs are shown in Fig. 2. The spherical shape of both drug-loaded and unloaded nanocarriers is observable.

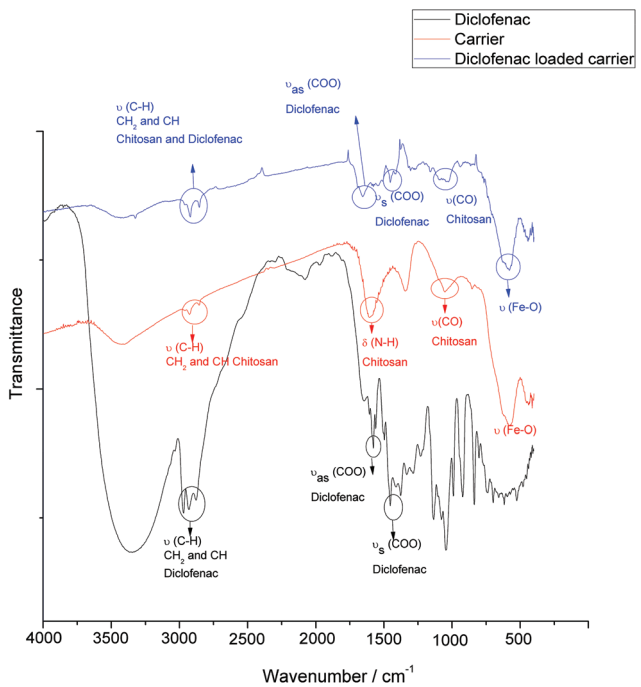

Fig. 1 FTIR-DRIFTS spectra corresponding to the diclofenac-loaded magnetic nanocarrier in comparison to the non-drug loaded nanosystem.

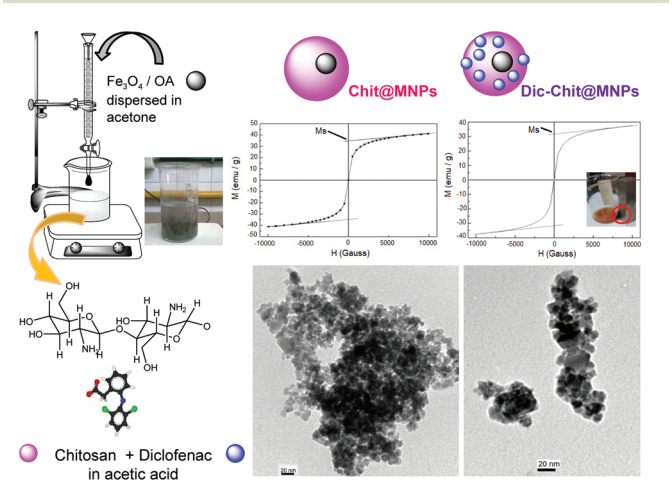

Fig. 2 Scheme of the synthesis procedure developed to obtain Chit@MMPs and Dic–Chit@MMPs. Magnetization and morphological characterization results for both the carrier and drug-loaded carrier.

The hydrodynamic diameter, obtained by DLS measurements in aqueous dispersions, was about 225 ± 5 nm for Dic–Chit@MNPs and 320 ± 4 nm for the unloaded magnetic carrier.

The surface charge resulted as positive for both nanocarriers, according to the zeta potential measurements: 34.0 mV for Dic–Chit@MNPs and 37.0 mV for Chit@MNPs.

Fig. 3 shows FTIR spectra of Dic–Chit@MNPs after 24 hours of incubation at pH 7.4 and 37 °C (physiological conditions) in the presence or absence of a magnetic field.

In Fig. 3, it is observed that in the spectra obtained from the sample exposed to the influence of the magnetic field, the bands corresponding to diclofenac [ν(CH_2 and CH) in the region near 2950 cm^{-1} and ν_{as}(COO) near 1650 cm^{-1}] are absent. This indicates that the complete drug release took place after 24 hours of incubation. In the region of 2950 cm^{-1} bands ascribed to ν(CH and CH_2) of chitosan are observed. These bands are misleading in the spectrum obtained after incubation with the magnet.

C.2. Effects of MNPs on endothelial cells

C.2.1. Effect of MNPs on endothelial NO production. The effect of different doses (1, 10 and 100 μg mL^{-1}) of the nanocarrier and the diclofenac-loaded carrier on NO production was examined. Fig. 4 shows that the presence of the MNPs did not affect basal NO production, since no statistically significant differences were detected between the control and treated groups. Acetylcholine is a physiological regulator of endothelial nitric oxide synthase (eNOS) that stimulates NO synthesis in a few minutes. In the presence of the nanocarrier (24 hours) the ability of ECs to respond to their natural agonist ACh was sustained. Similar results were observed when ECs were treated with different doses of the diclofenac-loaded magnetic nanodevice (Fig. 4A).

C.2.2. Effect of MNPs on endothelial cell viability. ECs were exposed to different doses (1, 10 and 100 μg mL^{-1}) of each nanodevice for 24 hours and cell viability was analyzed (Fig. 4B). No effect on cell viability was detected when ECs were treated with Chit@MNPs or Dic–Chit@MNPs, in comparison to control cells (100%). Only the cells exposed to the highest dose (100 μg mL^{-1}) of the diclofenac loaded carrier exhibited a significant difference in cell viability (43%) in comparison to the control. According to the images provided in Fig. 4C, the cell morphology was not affected by Chit@MNP or Dic–Chit@MNP treatment.

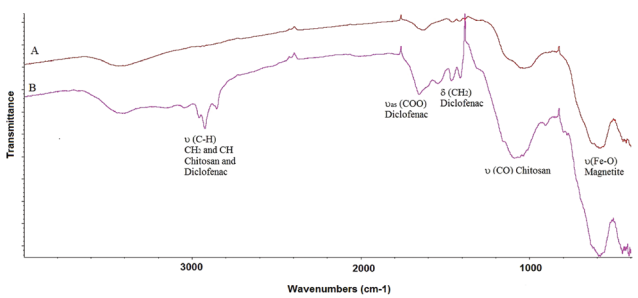

Fig. 3 FTIR spectra of Dic–Chit@MNPs after 24 hours of incubation at 37 °C in PBS buffer pH 7.4 to evaluate diclofenac release, under the influence of a magnetic field (A) and in the absence of a magnet (B).

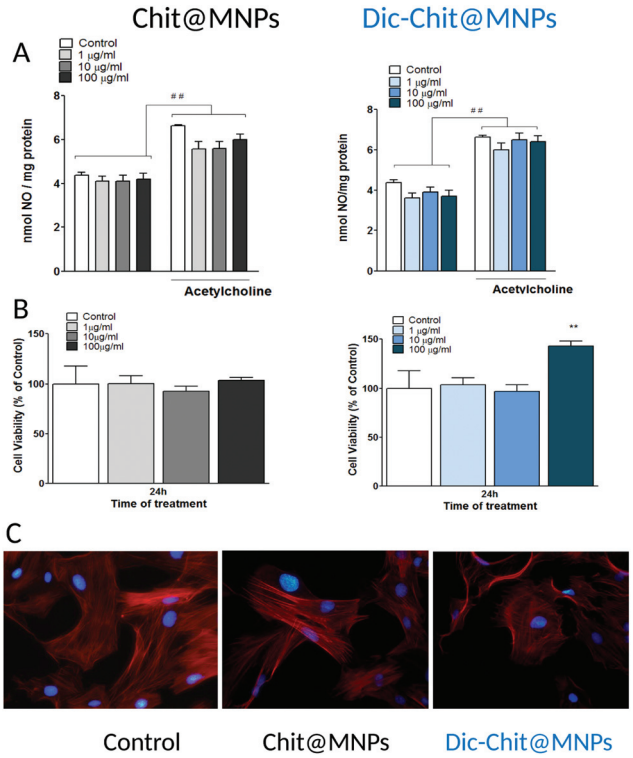

Fig. 4 A – Effects of the nanocarrier and the diclofenac-loaded nanocarrier on endothelial NO production. Endothelial cells were treated with magnetic nanoparticles (1, 10 and 100 μg mL^{-1}) for 24 hours. Immediately after treatment the monolayers were exposed to 10 μM Ach or a vehicle for 30 minutes. Results are expressed as mean ± S.D. $^{**}p < 0.01$ with respect to the control. $^{\#\#}p < 0.01$ without ACh *vs.* with ACh. B – Viability of endothelial cells incubated with Chit@MNPs and Dic–Chit@MNPs from three independent experiments. Cells were exposed to 1, 10 and 100 μg mL^{-1} of magnetic nanoparticles for 24 hours. Data are expressed as mean ± S.D. $^{**}p < 0.01$ *vs.* control. C – ECs exposed to 10 μg mL^{-1} MNP treatment. An Olympus BX41 microscope was used and images were recorded with an Olympus QColor 3 digital camera.

C.3. Hemocompatibility

The morphological analysis of human blood cells showed neither the deformation nor the decomposition of RBCs and white blood cells (WBCs) in the presence of the magnetic carriers at doses of 1 and 10 μg mL^{-1} (Fig. 5). Alterations in the membrane and in the morphology of RBCs were observed when blood was exposed to the 100 μg mL^{-1} dose of both MNPs.

Erythrocyte sedimentation rate (ESR) values, obtained after one hour exposure of anti-coagulated blood to increasing doses of 1, 10 and 100 μg mL^{-1} of Chit@MNPs or Dic–Chit@MNPs, are shown in Table 1. No significant differences in comparison to controls were observed.

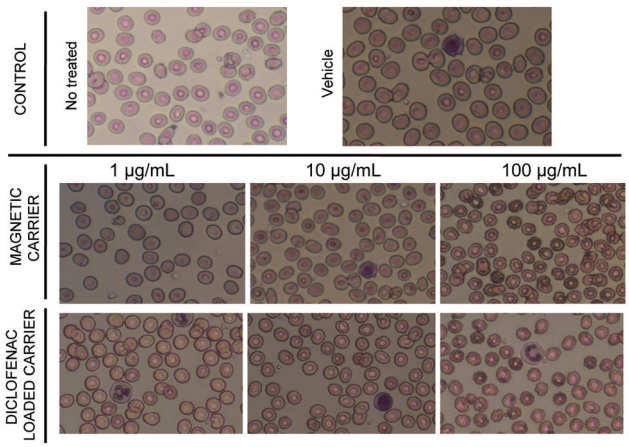

Fig. 5 OM images of the control and magnetic nanocarrier treated blood sample smears stained by May Grünwald-Giemsa staining. Samples were incubated at 37 °C for 40 minutes. Images were obtained with a phase contrast microscope (Nikon Eclipse TS100 coupled to a Nikon D3100 Camera) at a magnification of 40×.

Table 1 Erythrocyte sedimentation rate (ESR) of anti-coagulated peripheral blood exposed for 1 hour to increasing doses of the magnetic nanoparticles at room temperature. All conditions were processed by triplicate. Results are expressed as mean ± SD

1-Control without treatment; 2- Control treated with water; 3- Chit@MNPs 1 μg/mL; 4- Chit@MNPs 10 μg/mL; 5-Chit@MNPs 100 μg/mL; 6- Dic-Chit@MNPs 1 μg/mL; 7- Dic-Chit@MNPs 10 μg/mL; 8- Dic-Chit@MNPs 100 μg/mL

Control	
Without treatment	7 ± 2
With vehicle treatment (H_2O)	10 ± 3
Magnetic nanocarrier	
1 μg mL^{-1}	7 ± 1
10 μg mL^{-1}	7 ± 2
100 μg mL^{-1}	4 ± 2
Diclofenac-loaded magnetic nanocarrier	
1 μg mL^{-1}	6 ± 3
10 μg mL^{-1}	6 ± 1
100 μg mL^{-1}	6 ± 2

The hemolytic effect was not observed with any of the tested formulations and doses assayed, as observed in the RBC hemolysis experiment.

The MNP effect on platelet aggregation was assessed as described in the methodology. Aliquots of PRP were exposed to doses of 100 μg mL^{-1} of nano-magnetite, Chit@MNPs or Dic–Chit@MNPs (Fig. 6).

Platelet aggregation was not affected by the treatment with nano-magnetite. Chit@MNPs induced a slight decrease in platelet aggregation, while Dic–Chit@MNPs produced an inhibition of 28–32% (95% of confidence) with respect to the basal conditions.

C.4. Evaluation of different parameters of toxicity in mice

C.4.1. Functional observational battery for toxicity evaluation in mice for Chit@MNPs. Data obtained in the functional observational battery are shown in Table 2.

Mice exposed to Chit@MNPs did not present changes in the parameters evaluated in the home cage, in the hand-held observations nor during the manipulative test in comparison to the control group. Mice treated with the nanocarrier exhibited a significant decrease in the number of urine pools deposited compared to the control ($p < 0.01$). No significant changes in the number of fecal boluses with respect to the control group were observed. Sensorial responses were ranked according to a variety of stimuli as described in the methodology. The parameters evaluated in the open field arena were not altered in either of the experimental groups.

C.4.2. Histopathological analysis. The histopathological examinations of the liver, stomach, intestine, lungs and brain showed no changes with hematoxylin–eosin at the end of the sub-acute exposure to the nanocarrier in any of the mice after 28 days of the assay. The kidneys of all the animals exposed to the magnetic carrier exhibited granular interstitial tissue, compatible with periarteriolar interstitial nephritis in comparison to the control group as it can be seen in Fig. 7. When the spleen was analyzed in mice exposed to the nanodevice, an increase in the presence of megakaryocytes was observed (up

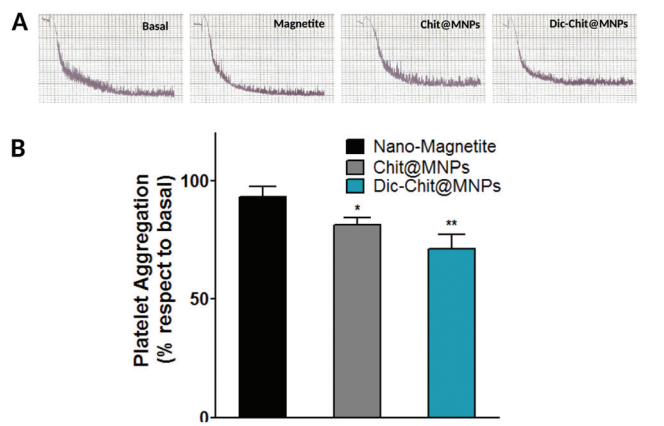

Fig. 6 A – Platelet aggregation curves. B – platelet aggregation expressed as % with respect to the basal for both, unloaded and diclofenac loaded MNPs. Nano-magnetite was also assayed to evaluate the effect of the iron core in the process. *$p < 0.05$ with respect to basal; **$p < 0.01$ with respect to basal.

Table 2 Parameters evaluated in the functional observational battery

Endpoints	Control	Chit@MNPs
Home cage observations		
Normal body posture (D)	100	100
Activity (R)	2.50	2.50
Palpebral closure (R)	1.00	1.00
Clonic movements (D)	0	0
Tonic movements (D)	0	0
Biting (D)	0	0
Vocalizations (B)	0	0
Hand-held observations		
Ease of removal from cage (R)	1.00	1.00
Ease of handling (R)	2.63	2.50
Salivation (R)	1.00	1.00
Lacrimation (R)	1.00	1.00
Piloerection (B)	0	0
Normal fur appearance (D)	100	100
Normal respiration (D)	100	100
Normal cardiovascular signs (D)	100	100
Normal limb tone (D)	100	100
Normal abdominal tone (D)	100	100
Limb grasping (B)	100	100
Open field observations		
Activity level (R)	2.30	2.10
Rearing (R)	1.06	1.06
Arousal (R)	3.20	3.10
Normal gait (D)	100	100
Unusual movements (D)	1.00	1.00
Stereotyped behaviors (D)	1.00	1.00
Pelvic elevation (R)	3.00	3.00
Normal tail position (D)	100	100
Fecal boluses (C)	3.75	4.40
Urine pools (C)	1.00	0.40**
Diarrhea (B)	0	0
Sensory reflexes		
Approach response (R)	2.00	2.00
Touch response (R)	2.00	2.00
Click response (R)	2.00	2.00
Tail pinch response (R)	2.06	2.06
Palpebral reflex (B)	100	100
Pinna reflex (B)	100	100
Motor reflexes		
Flexor reflex (B)	100	100
Extensor reflex (B)	100	100
Rigthing reflex (R)	1.00	1.00
Landing foot splay (C)	4.20	4.20
Wire maneuver (R)	1.00	1.00

**$p < 0.01$ with respect to the control. Descriptive (D) and binary (B) data, expressed as percentages of incidence (chi-square test); ranked (R) data, expressed as the mean score of the scale used (Kruskal–Wallis test); continuous (C) data, expressed as the mean value (One-way ANOVA test) $n = 8$. Procedural details and scoring criteria for the functional observational battery protocol were performed according to Moser and Ross[25] and modified for mice.[26,27]

to 5 per field), compared to the control (up to 2 per field) (see Fig. 7).

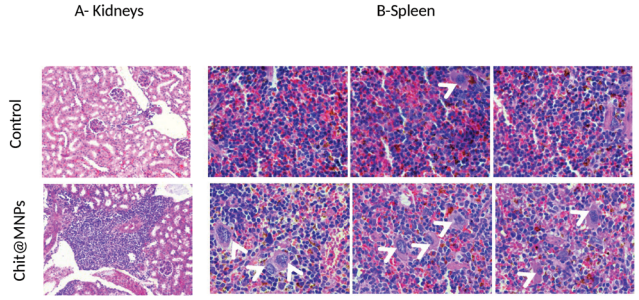

Fig. 7 Representative micrographs of kidney (A) and spleen (B) sections (5 μm thick) stained with hematoxylin–eosin corresponding to mice treated with a dose of 30 mg kg^{-1} of the magnetic nanocarrier, in comparison to the control. Arrows indicate megakaryocytes in the spleen.

D. Discussion

A simple two-step synthesis procedure has been designed to obtain a drug-loaded functionalized magnetic nanocarrier. The synthesis protocol resulted in an improvement in the encapsulation efficiency and promoted a satisfactory level of drug loading.

In previous work we have extensively studied the experimental conditions and mechanisms involved in diclofenac adsorption on magnetic nanocarriers functionalized with chitosan. In the first study we obtained a formulation constituted by magnetite coated with chitosan, achieving a Diclofenac Loading Efficiency(DLE) estimated as 54%.[11] Chitosan was then crosslinked with glutaraldehyde to improve the stability of the formulation, reaching a higher level of drug incorporation. By this procedure, we obtained a nanosized formulation with a DLE of 33%.[12] The main difference of this formulation with respect to the earlier published ones is related to the encapsulation method. Here, we intend to improve DLE, and to this end, the incorporation of the NSAID was conducted in an earlier step, where diclofenac was allowed to interact directly with the chitosan (Fig. 1). This encapsulation procedure rendered 84.0% of DLE, which represents a great improvement regarding the adsorption methods previously employed. It is worth mentioning that reliable DLE values were reached by the implementation of a quantification method that minimizes the error sources. In fact the widely used UV/visible technique to measure diclofenac in the supernatant was not suitable in this case due to interferences arising from chitosan disaggregation on the MNP surface. The quantification method used within this work was earlier employed by other researchers[13] for diclofenac detection in complex matrixes.

The early and direct interaction between diclofenac and chitosan would be critical to achieve a satisfactory drug encapsulation. The mechanism by which the diclofenac remains linked to the polymeric chains may be inferred on the basis of the characterization results, in particular from zeta potential data.

The pH value registered at the end of this first step of the synthesis procedure was 5. Thereby, electrostatic interactions may occur between the anionic carboxylate group ($-COO^-$) of diclofenac (pK_a 3.8) and positive amino protonated groups of

chitosan ($-NH_3^+$) (isoelectric point 6.3).[28] The promotion of interactions between the NSAID and the biopolymer was a satisfactory strategy to increase drug incorporation into the nanocarrier.

The addition of a nano-magnetite dispersed in acetone to the chitosan–diclofenac reaction medium, raised the pH to 5.5.

Thus, the nanoprecipitation of chitosan over the magnetite surface takes place by interaction of the iron oxide and the positively-charged amino groups of chitosan that were not compromised in the interactions with diclofenac, leaving the surface exposed.

The positive ζ value of aqueous dispersions of Dic–Chit@MNPs revealed a positively charged surface. In previous studies, we have demonstrated that the ζ of a dispersion of magnetic nanoparticles composed of magnetite-oleic acid and coated with chitosan may be considerably different depending on the concentration of a biopolymer linked to the nanoparticle surface.[29] These results indicate that the synthesis procedure renders a complete chitosan coating of the nano-magnetite surface. It is worth noting that the magnitude of ζ is almost the same in both nanocarriers, suggesting that diclofenac would remain in the inner core of the nanocarrier between magnetite and chitosan.

Regarding the magnetic properties it was noticed that the presence of diclofenac did not affect the magnetic behaviour of nanocarriers. This conclusion emerged after the analysis of M_s values for both formulations. This finding is essential for the practical implementation of these nanosystems for drug targeting to a specific site of the body by the employment of an external magnetic field.

Drug release from Dic–Chit@MNPs was analyzed by FTIR. The absence of bands corresponding to diclofenac in the remaining sample exposed to the magnet indicates that it was completely released from the structure of the nanocarrier after 24 hours. Moreover, misleading bands corresponding to chitosan would indicate that the biopolymer would also disaggregate from the MNP surface. These results are consistent with the mechanism proposed for drug–nanocarrier interactions. On the other hand, in the sample that was not exposed to a magnetic field, diclofenac remained inside MNPs after a 24-hour release study.

On the basis of these results it can be inferred that the presence of a magnetic field may induce changes in magnetite, modifying interactions with the coating and with the loaded drug. Hence, the presence of a magnetic field may be considered to be stimuli induced or modifying the release kinetic and mechanism. Further studies will be necessary to elucidate the mechanisms involved in diclofenac release from MPNs in the presence of a magnetic field.

The main goal of the present research is to assess the most relevant aspects of the possible systemic effects of chitosan-coated MNPs. Once the MNPs enter the bloodstream, they are exposed to the formed elements of blood such as red blood cells (RBCs) and platelets. Thus, the study of the impact of MNPs on blood components and on the endothelium (the first barrier that particles must overcome to get their target) is extremely important to determine their potential toxicity.

Nanoparticles intended for biomedical applications must be essentially hemo-compatible, since the blood circulation system is the first pathway to achieve an efficient target to blank organs or tissues.

Four *in vitro* assays were performed on human blood to assess the hemocompatibility of Chit@MNPs and Dic–Chit@MNPs: a study of the blood cell morphology (microscopy analysis of blood smears), ESR, hemolysis and platelet aggregation. RBC sedimentation in the presence of the MNPs was evaluated by the Westergren ESR method. This method evaluates the rate at which RBCs sediment in a period of one hour. ESR is an indirect measure of pro-sedimentation factors (mainly fibrinogen and immunoglobulins) and anti-sedimentation factors, such as the negative surface charge of erythrocytes (zeta potential). Normal values of the Z potential for healthy subjects below 50 years old are up to 15 mm h^{-1} for men and 20 mm h^{-1} for women.[30] The results of the ESR assay for both studied MNPs were within the normal range. The hemolytic effect of both formulations of MNPs at the doses studied can be considered as insignificant, since free Hb levels were below the detection limit of the assay.

Scarce research studies dedicated to the study of the impact of MNPs on RBCs may be found in the available literature. Different coatings for the iron oxide core of MNPs have been explored and were not found to cause deformation or decomposition of RBCs, including poly-acids,[31,32] dehydroascorbic acid (DHA),[33] and oleate double layered and coated with polyethylene glycol (PEG).[34] In the study performed by Drašler *et al.*[35] it was found that citric acid (CA) coated magnetic cobalt ferrite ($CoFe_2O_4$) nanoparticles induced a significant increase of burr-shaped RBCs that was not observed with bare $CoFe_2O_4$ nanoparticles. This finding is consistent with smaller sized agglomerates of CA-adsorbed $CoFe_2O_4$ which would react with lipid membranes. Thus, the coating would be an important factor, determinant of MNP biocompatibility.

The present research is one of the first studies devoted to the evaluation of chitosan-coated MNP toxicity on RBCs and platelets. Jayalekshmi *et al.*[36] synthesized iron oxide incorporated into chitosan-gelatin bioglass composite nanoparticles as drug carriers for hyperthermia treatment. The authors performed qualitative studies on blood compatibility. The RBC and WBC morphology and platelet aggregation were not affected by incubation with the composite.

There are many factors associated with the effects of nanoparticles on cell membranes such as:

1 – the interactions induced by surface charge[35] and 2 – adsorption of nanoparticles to the lipid component of the membrane or to membrane-bound proteins. The contact of MNPs with RBC membrane phospholipids would cause an expansion of the inner to the outer leaflet resulting in membrane shape transformation.[37] Electrostatic interactions between Dic–Chit@MNPs or Chit@MNPs with RBCs are possible through the positive surface charge of chitosan and the negative charge of the RBC surface. The research performed by

Dodane and Vilivalam[38] demonstrated that chitosan has membrane perturbing properties but does not decrease cell viability as it was informed in their study. Thus, the chitosan coating would be responsible for the alterations in the RBC membrane at the highest dose of 100 μg mL^{-1} as it was observed in smears. At lower MNP doses, the chitosan concentration would not be high enough to induce changes in the cell morphology.

No adsorption of the MNPs on the membrane of RBCs was observed in the smears. Doses up to 10 μg mL^{-1} of both Chit@MNPs and Dic–Chit@MNPs would be safe for RBCs, allowing the effective application of these nanosystems as drug carriers.

Platelets constitute blood cellular components responsible for the coagulation process and essential for homeostasis maintenance.[39,40] Thrombogenic effects of new biomedical materials are often studied by the evaluation of platelet aggregation *in vitro* as part of hemocompatibility features. Contradictory data related to thrombogenic properties of nanomaterials have been found in the current literature.[41] The size, surface charge or composition of nanoparticles may be responsible for thrombogenic properties. In general, it has been demonstrated that MNPs alter the coagulation process by diverse mechanisms. One of them is related to the possible oxidative stress exerted by iron. Smaller iron MNPs have been proven to alter the plasma coagulation parameters rather than larger particles.[42] The effect of the nanocarriers here presented on platelets was assessed by studying their effect on ADP induced platelet aggregation. In this research work we have contrasted experiments with the bare nanomagnetite core to better understand the results. In this regards, no effect on platelet aggregation was observed for oleic acid-coated nanomagnetite. This indicates that iron would not produce alterations in this process. Chou *et al.*[43] demonstrated that chitosan enhances platelet adhesion and aggregation while Li *et al.*[44] showed that chitosan coated MNPs did not modify platelet aggregation below 10 μg mL^{-1}. In this way, nanotechnology applied to chitosan would reduce its side effects on platelet aggregation. Dic–Chit@MNPs significantly decreased platelet aggregation, which is due to diclofenac, considering it as an inhibitor of platelet aggregation by diverse mechanisms.[45] Among these mechanisms, the induction of increased negative charges on the platelet membrane, increasing repulsive forces among platelets, is the most relevant.[46] The slight decrease in platelet aggregation induced by Chit@MNPs could be ascribable to this mechanism due to possible diclofenac release but further research is necessary to test this hypothesis. The present results demonstrate the non-thrombogenic property of these MNPs, which is an indispensable condition for biomedical applications.

The study performed on rat aortic EC cultures showed that endothelial NO production was not affected by the exposure to Chit@MNPs or Dic–Chit@MNPs. Treatment with both MNPs did not cause alterations on the response of the cells to the endogenous agonist ACh.

The endothelial production of NO is one of the major important markers of EC function. NO is one of the most important bioactive molecules and is a key factor for the regulation of the vascular tone and the maintenance of homeostasis. It is synthesized by the conversion of L-arginine to L-citrulline, a reaction that is catalyzed in ECs by the eNOS. This process is physiologically regulated by vascular agonists such as acetylcholine, bradykinin, and diverse hormones and it is critical to the maintenance of healthy properties of the vascular wall.[47] A decrease in NO production by ECs is an indicator of endothelial dysfunction. The presence of the MNPs did not alter the basal production of NO nor the ability of the cells to respond to their endogenous agonist (ACh). Indeed, no differences in the cell morphology were detected either on evaluation by phase contrast microscopy or by actin cytoskeleton staining. Cell viability was assessed by the 3-[4,5-dimethylthiazol-2-yl]-2,5-diphenyltetrazolium bromide (MTT) assay. This method evaluates mitochondrial activity as an indicator of cell viability, since only living cells are capable of reducing MTT to formazan (which is the colorimetric end product of the reaction that is quantified).[48] The treatment of ECs for 24 hours with Chit@MNPs did not affect cell viability in the applied doses. The highest dose of Dic–Chit@MNPs (100 μg mL^{-1}) induced a significant decrease in EC viability with respect to the control.

The difference may be ascribable to the release of diclofenac. This drug is a non-selective COX inhibitor (inhibits cyclooxygenase-1 and 2) blocking the formation of prostaglandins (PGs). A similar antiproliferative effect on ECs was described for other COX inhibitors like sulindac,[49] aspirin[50] and celecoxib.[51] Wiktorowska-Owczarek demonstrated that diclofenac inhibits human endothelial cell (HMEC-1) viability by inhibiting prostaglandin synthesis.[52] Cytotoxicity measurements indicate that Chit@MNPs do not exert alterations on the metabolism and integrity of ECs in doses up to 100 μg mL^{-1}. This feature makes this magnetic carrier suitable for biomedical applications.

The systemic toxicity of a given chemical agent depends on many factors such as the chemical structure, the dose level, the method of administration, the duration of the treatment period, the pharmacokinetics and metabolism. Because of this, we evaluated the effects of a sub-acute exposure of Chit@MNPs as a potential drug carrier. A dose of 30 mg kg^{-1} was chosen for the *in vivo* assay on mice, a concentration that could be used for patients in clinical trials. After 28 days of exposure different parameters of toxicity were evaluated: the behavioral and functional nervous system parameters in a functional observational battery. No significant differences were found in comparison to the control group. Mice exposed to Chit@MNPs did not show signs of neurobehavioral alterations in the period of time of the study. In concordance, no alterations in brain tissue were observed by histological examination. These results suggest that Chit@MNPs do not exert significant adverse effects on behavioral and functional nervous system parameters related to neurobehavioral toxicity.

The group exposed to Chit@MNPs presented a reduced number of urine pools, suggesting a possible renal damage. This finding is in accordance with the histopathological study of kidneys from treated mice which revealed the presence of abnormal areas compatible with periarteriolar nephritis. Kidneys are vital organs involved in electrolyte regulation, excretion and blood pressure control. They also produce hormones such as calcitriol, erythropoietin and renin.[53] Nephritis is a rather uncommon disease of the kidney associated with an inflammatory response. Drugs are the main triggers of this pathology. There exist different mechanisms whereby a drug or metabolite can induce nephritis. The deposition within the interstitium is a way to act as a trapped antigen and trigger an inflammatory reaction. Chit@MNPs deposited in the periarteriolar zone may cause inflammation leading to nephritis. The mechanism by which this process occurs may be associated with the magnetic core and not to the chitosan coating. Onishi *et al.* reported that after IP administration in mice the chitosan was predominantly localized in the kidney after 1 hour.[54] It presented a rapid renal excretion. Thus, chitosan coating may be lost in the kidney without toxic effects and the deposition of magnetite would be the responsible for the local inflammation. Feng *et al.* reported biochemical and physiological perturbations in a study developed on mice, associated with renal toxicity induced by ultrasmall superparamagnetic particles of iron oxides (USPIONs).[55] Uncoated USPIONs were absorbed by kidneys inducing "local effects". Ma *et al.*[56] detected oxidative stress markers in the kidneys of mice administered with different doses of nano-magnetite.

MNP treatment did not cause a distortion of the spleen architecture, although an increased accumulation of splenic megakaryocytes was detected. Megakaryocytes are specialized cells responsible for the production of platelets.[57] An increase of splenic megakaryocytes indicates an extramedullary hematopoietic process associated with pathological conditions.[58] No other signs of tissue alterations such as inflammation or alterations in the spleen architecture were found. Chitosan coating would prevent the development of spleen tissue inflammation since no sign of macrophage or lymphocyte infiltration was observed.

Awaad *et al.* studied the impact of uncoated MNPs prepared by a sol–gel method following intravaginal instillation on the spleen, liver and genital tract of female mice.[59] It was found that there was an increase in the number of megakaryocytes in the spleen. Furthermore, a higher number of splenic lymphocytes were also observed, presenting marginal and vacuolated chromatin, attributable to the presence of iron. No additional reports are available in the literature about the histological effect of MNPs on the spleen. The underlying mechanisms associated with the spleen toxicity of MNPs remain to be elucidated.

Previous research[60] revealed that the accumulation of MNPs in the lung would induce inflammatory reactions by oxidative stress promoted by iron toxicity. Chitosan coating may prevent potential iron toxicity in Chit@MNPs as no signs of inflammation were observed in the histopathological assays.

E. Concluding remarks

A simple two-step drug encapsulation method was satisfactorily applied to develop a biocompatible magnetic nanocarrier with improved loading efficiency and acceptable drug release for biomedical applications. A comprehensive analysis of the factors implied in the therapeutic and toxicological concerns of the MNPs obtained as drug delivery devices in relation to physico-chemical properties revealed that chitosan coating resulted as a key for the biocompatibility of the systems. While the results of hemocompatibility, and vascular and neurobehavioral toxicity were satisfactory, we must not lose sight of future biomedical applications as the nanocarrier generated renal toxicity and indications of possible splenic disorders. Kidneys would not be a possible target organ for treatment with these nanodevices, at least as designed.

Further research is underway regarding the magnetic targeting of these nanocarriers to different organs and the evaluation of the therapeutic action of diclofenac once released. Anyway, the general knowledge on systemic toxicity results is crucial for providing biomedical insights.

Acknowledgements

The authors thank CONICET and UNS for financial support.

Notes and references

1 K. Hola, Z. Markova, G. Zoppellaro, J. Tucek and R. Zboril, *Biotechnol. Adv.*, 2015, **6**(Pt 2), 1162–1176.
2 J. Kolosnjaj-Tabi, L. Ã. Lartigue, Y. Javed, N. Luciani, T. Pellegrino, C. Wilhelm, D. Alloyeau and F. Gazeau, *Nano Today*, 2016, **11**, 280.
3 M. Ferrari, *Nat. Rev. Cancer*, 2005, **3**, 161–171.
4 G. Tang, K. Ding, Z. Nikolovska-Coleska, C. Y. Yang, S. Qiu, S. Shangary, R. Wang, J. Guo, W. Gao, J. Meagher, J. Stuckey, K. Krajewski, S. Jiang, P. P. Roller and S. Wang, *J. Med. Chem.*, 2007, **14**, 3163–3166.
5 M. Arruebo, R. Fernández-Pacheco, M. R. Ibarra and J. Santamaria, *Nano Today*, 2007, **3**, 22–32.
6 M. Hofmann-Amtenbrink, H. Hofmann and X. Montet, *Swiss Med. Wkly.*, 2010, w13081.
7 D. M. Huang, T. H. Chung, Y. Hung, F. Lu, S. H. Wu, C. Y. Mou, M. Yao and Y. C. Chen, *Toxicol. Appl. Pharmacol.*, 2008, **2**, 208–215.
8 P. Frank and M. A. Ottoboni, *The Dose Makes the Poison: A Plain-Language Guide to Toxicology*, Wiley, 3rd edn, 2011.
9 J. S. Kim, T. J. Yoon, K. N. Yu, B. G. Kim, S. J. Park, H. W. Kim, K. H. Lee, S. B. Park, J. K. Lee and M. H. Cho, *Toxicol. Sci.*, 2006, **1**, 338–347.
10 J. E. Kim, J. Y. Shin and M. H. Cho, *Arch. Toxicol.*, 2012, **5**, 685–700.
11 M. Agotegaray, S. Palma and V. Lassalle, *J. Nanosci. Nanotechnol.*, 2014, **5**, 3343–3347.

12 M. Agotegaray and V. Lassalle, *Int. J. Chem. Pharm. Anal.*, 2014, **4**, 154–164.
13 A. A. Matin, M. A. Farajzadeh and A. Jouyban, *Farmaco*, 2005, **10**, 855–858.
14 National Research Council, *Guide for the Care and use of Laboratory Animals*, National Academies Press, Washington, DC, 2011.
15 Y. C. Yeh, G. Y. Hwang, I. P. Liu and V. C. Yang, *Atherosclerosis*, 2002, **1**, 95–103.
16 A. E. Campelo, P. H. Cutini and V. L. Massheimer, *Steroids*, 2012, **11**, 1033–1040.
17 A. E. Campelo, P. H. Cutini and V. L. Massheimer, *J. Endocrinol.*, 2012, **1**, 77–87.
18 O. H. Lowry, N. J. Rosebrough, A. L. Farr and R. J. Randall, *J. Biol. Chem.*, 1951, **1**, 265–275.
19 P. H. Cutini, A. E. Campelo and V. L. Massheimer, *J. Endocrinol.*, 2014, **3**, 179–193.
20 A. Westergren, *Triangle*, 1957, **1**, 20–25.
21 E. Van Kampen and W. G. Zijlstra, *Clin. Chim. Acta*, 1961, 538–544.
22 V. Massheimer, N. Polini, C. Alvarez, S. Benozzi and J. Selles, *Maturitas*, 2002, **1**, 55–64.
23 N. Polini, M. B. Rauschemberger, J. Mendiberri, J. Selles and V. Massheimer, *Mol. Cell. Endocrinol.*, 2007, **1–2**, 55–62.
24 K. Kikuta, T. Sawamura, S. Miwa, N. Hashimoto and T. Masaki, *Circ. Res.*, 1998, **11**, 1088–1096.
25 M. L. Moser, S. W. Ross and K. J. Sulak, *Mar. Ecol.: Prog. Ser.*, 1996, 57–61.
26 K. Ingman, J. Sallinen, A. Honkanen and E. R. Korpi, *Pharmacol., Biochem. Behav.*, 2004, **4**, 847–854.
27 A. F. Youssef and B. W. Santi, *Environ. Res.*, 1997, **1–2**, 52–62.
28 J. Zhang, W. Xia, P. Liu, Q. Cheng, T. Tahirou, W. Gu and B. Li, *Mar. Drugs*, 2010, **7**, 1962–1987.
29 P. Nicolas, M. Saleta, H. Troiani, R. Zysler, V. Lassalle and M. L. Ferreira, *Acta Biomater.*, 2013, **1**, 4754–4762.
30 V. Corrons and J. L. Bascompte, *Manual de Técnicas de laboratorio en hematología*, Masson, España, 2006.
31 M. Szekeres, I. Y. Toth, E. Illes, A. Hajdu, I. Zupko, K. Farkas, G. Oszlanczi, L. Tiszlavicz and E. Tombacz, *Int. J. Mol. Sci.*, 2013, **7**, 14550–14574.
32 M. Ã. Szekeres, E. b. Illés, C. Janko, K. Farkas, I. Y. Tóth, D. Ã. Nesztor, I. N. Zupkó, I. Földesi, C. Alexiou and E. Tombácz, *J. Nanomed. Nanotechnol.*, 2015, 2015, DOI: 10.4172/2157-7439.1000252.
33 H. Gupta, P. Paul, N. Kumar, S. Baxi and D. P. Das, *J. Colloid Interface Sci.*, 2014, 221–228.
34 E. Illés, M. Szekeres, E. Kupcsik, I. Y. Tóth, K. Farkas, A. Jedlovszky-Hajdú and E. Tombácz, *Colloids Surf., A*, 2014, 429–440.
35 B. Drašler, D. Drobne, S. Novak, J. Valant, S. Boljte, L. Otrin, M. Rappolt, B. Sartori, A. Iglic, V. Kralj-Iglic, V. Sustar, D. Makovec, S. Gyergyek, M. Hocevar, M. Godec and J. Zupanc, *Int. J. Nanomed.*, 2014, 1559–1581.
36 A. C. Jayalekshmi, S. P. Victor and C. P. Sharma, *Colloids Surf., B*, 2013, 196–204.
37 S. V. Rudenko, *Biochim. Biophys. Acta*, 2010, **9**, 1767–1778.
38 V. r. Dodane and V. D. Vilivalam, *Pharm. Sci. Technol. Today*, 1998, **6**, 246–253.
39 J. Simak, *Nanotoxicity: From in vivo and in vitro models to health risks*, John Wiley & Sons, Chichester, 2009, pp. 191–225.
40 J. Simak, in *Nanotoxicity: From In Vivo to an In Vitro Models to Health Risks*, ed. S. Sahu and D. Casciano, John Wiley and Sons, 2009, pp. 191–225.
41 M. A. Dobrovolskaia, A. K. Patri, J. Simak, J. B. Hall, J. Semberova, S. H. De Paoli Lacerda and S. E. McNeil, *Mol. Pharm.*, 2012, **3**, 382–393.
42 A. N. Ilinskaya and M. A. Dobrovolskaia, *Nanomedicine*, 2013, **6**, 969–981.
43 T. C. Chou, E. Fu, C. J. Wu and J. H. Yeh, *Biochem. Biophys. Res. Commun.*, 2003, **3**, 480–483.
44 X. Li, A. Radomski, O. I. Corrigan, L. Tajber, M. F. De Sousa, S. Endter, C. Medina and M. W. Radomski, *Nanomedicine*, 2009, **7**, 735–746.
45 P. A. Todd and E. M. Sorkin, *Drugs*, 1988, **3**, 244–285.
46 M. Djaldetti, P. Fishman, A. Cohen, E. Roffman, H. Levinsky, M. Glaser and I. Zahavi, *Acta Haematol.*, 1983, **5**, 296–301.
47 C. Michiels, *J. Cell Physiol.*, 2003, **3**, 430–443.
48 T. Mosmann, *J. Immunol. Methods*, 1983, **1–2**, 55–63.
49 S. Narendra, S. Venkataramani, G. Shen, J. Wang, V. Pasapula, Y. Lin, D. Kornyeyev, A. S. Holaday and H. Zhang, *J. Exp. Bot.*, 2006, **12**, 3033–3042.
50 Q. Q. Chen, W. L. Liu, X. Guo, Y. J. Li and Z. G. Guo, *Acta Pharmacol. Sin.*, 2007, **3**, 353–358.
51 E. Niederberger, C. Manderscheid, S. Grosch, H. Schmidt, C. Ehnert and G. Geisslinger, *Biochem. Pharmacol.*, 2004, **2**, 341–350.
52 A. Wiktorowska-Owczarek, *Acta Pharm.*, 2014, **1**, 131–138.
53 Jk. E. Hall, *Guyton and Hall textbook of medical physiology*, 2015.
54 H. Onishi and Y. Machida, *Biomaterials*, 1999, **2**, 175–182.
55 J. Feng, H. Liu, K. K. Bhakoo, L. Lu and Z. Chen, *Biomaterials*, 2011, **27**, 6558–6569.
56 P. Ma, Q. Luo, J. Chen, Y. Gan, J. Du, S. Ding, Z. Xi and X. Yang, *Int. J. Nanomed.*, 2012, 4809–4818.
57 E. C. Josefsson, C. James, K. J. Henley, M. A. Debrincat, K. L. Rogers, M. R. Dowling, M. J. White, E. A. Kruse, R. M. Lane, S. Ellis, P. Nurden, K. D. Mason, L. A. O'Reilly, A. W. Roberts, D. Metcalf, D. C. Huang and B. T. Kile, *J. Exp. Med.*, 2011, **10**, 2017–2031.
58 Y. Yu, Y. Li, W. Wang, M. Jin, Z. Du, Y. Li, J. Duan, Y. Yu and Z. Sun, *PLoS One*, 2013, **4**, e61346.
59 A. Awaad, *J. Basic Appl. Zool.*, 2015, 32–47.
60 S. S. Nigavekar, L. Y. Sung, M. Llanes, A. El-Jawahri, T. S. Lawrence, C. W. Becker, L. Balogh and M. K. Khan, *Pharm. Res.*, 2004, **3**, 476–483.